

## Review

## Multimodal neural probes for combined optogenetics and electrophysiology

Huihui Tian,<sup>1</sup> Ke Xu,<sup>1,2,3</sup> Liang Zou,<sup>1,2,3</sup> and Ying Fang<sup>1,2,3,\*</sup>

## SUMMARY

To understand how brain functions arise from interconnected neural networks, it is necessary to develop tools that can allow simultaneous manipulation and recording of neural activities. Multimodal neural probes, especially those that combine optogenetics with electrophysiology, provide a powerful tool for the dissection of neural circuit functions and understanding of brain diseases. In this review, we provide an overview of recent developments in multimodal neural probes. We will focus on materials and integration strategies of multimodal neural probes to achieve combined optogenetic stimulation and electrical recordings with high spatiotemporal precision and low invasiveness. In addition, we will also discuss future opportunities of multimodal neural interfaces in basic and translational neuroscience.

## INTRODUCTION

Human central nervous system consists of billions of neurons that are of various types and interconnected through trillions of connections to form a multitude of neural networks, making the brain a powerful information processor (Herculano-Houzel, 2009). A central goal of neuroscience is to understand how animal behaviors are controlled by neural circuit activities (Frank et al., 2019; Kuo et al., 2018; Vázquez-Guardado et al., 2020). To achieve this goal, it is necessary to develop multimodal tools that are capable of manipulating and recording the activities of specific types of neurons at high spatiotemporal resolution. Moreover, the development of multimodal neural interfaces offers important opportunities in translational and clinical research, such as the treatment of neurological disorders and brain-computer interfaces (BCIs).

Conventional neural modulation approaches include electrical stimulation through implanted depth electrodes and pharmacological modulation through systemic perfusion or localized cannula injection into targeted brain regions. Electrical stimulation can activate neural activities at millisecond resolution and has been one of the most widely applied tools in basic and clinical applications, such as seizure control and bradykinesia relief in Parkinson disease. However, electrical stimulation lacks cell-type specificity (Borchers et al., 2012; Chen et al., 2017). Meanwhile, high current density is sometimes required to elicit a response during electrical stimulation, which can produce excessive heat and cause tissue damage at electrode-tissue interface (Cogan, 2008). Pharmacological modulation can allow for cell-type specific activation or inhibition of neural activities. However, pharmacological modulation is limited by poor temporal and spatial resolution due to the slow and diffusive nature of drug delivery (Won et al., 2020).

Optogenetics combines genetic and optical methods to control neural activities with light (Deisseroth, 2011; Han et al., 2009; Paoletti et al., 2019; Pastrana, 2011). In optogenetics, genetic methods are utilized to selectively express light-sensitive opsins, including excitatory channelrhodopsin (e.g. ChR2) and inhibitory halorhodopsin (e.g. NpHR), in specific types of cells (Chen et al., 2021; Deisseroth, 2015; Gradinaru et al., 2008; Zhang et al., 2010). Light activation of these opsins can activate or inhibit cellular excitability at millisecond precision (Arenkiel et al., 2007; Boyden et al., 2005; Zhang et al., 2008). As a result, optogenetics can modulate neural activities with both cell-type specificity and high temporal precision, which is unattainable with traditional electrical stimulation or pharmacologic modulation (Chen et al., 2017; Tehovnik, 1996; Vázquez-Guardado et al., 2020). Over the past decade, optogenetics has significantly improved our understanding of not only neural circuit functions underlying natural behaviors but also the synaptic and neuronal defects that lead to neurological disorders (Gradinaru et al., 2009; Kim et al., 2017; Kohara et al., 2014; O'Shea et al., 2018; Tsai et al., 2009; Tye et al., 2011; Tye and Deisseroth, 2012; Won et al., 2020).

<sup>1</sup>CAS Center for Excellence in Nanoscience, National Center for Nanoscience and Technology, Beijing 100190, China

<sup>2</sup>CAS Center for Excellence in Brain Science and Intelligence Technology, Institute of Neuroscience, Chinese Academy of Sciences, Shanghai 200031, China

<sup>3</sup>University of Chinese Academy of Sciences, Beijing 100049, China

\*Correspondence: fangy@nanoctr.cn

<https://doi.org/10.1016/j.isci.2021.103612>



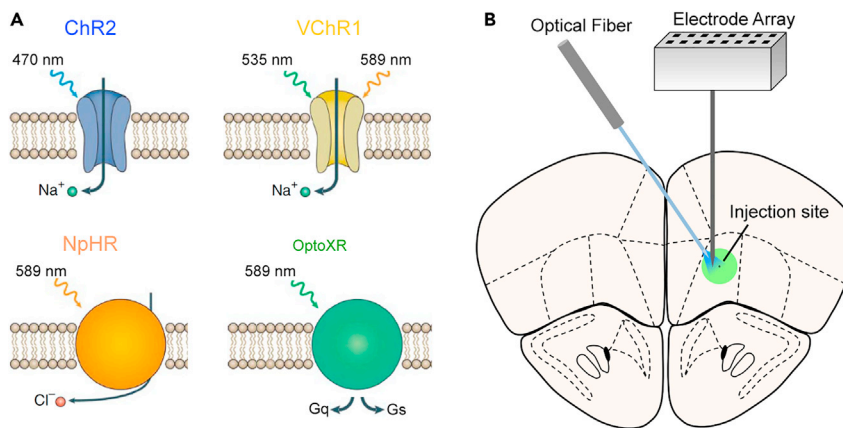


**Figure 1. Combined optogenetics/electrophysiology in the Brain**

(A) Optogenetic tool families: ChR2 from *Chlamydomonas reinhardtii* and VChR1 from *Volvox carteri*, which are cation-conducting channels; NpHR from *Natronomonas pharaonis*, which is a chloride pump; optoXR is engineered synthetic rhodopsins for the optical control of well-defined intracellular biochemical signaling. Useful light wavelengths for each are indicated. Panel A is reproduced from Zhang et al. (2010).

(B) Schematic of combined optogenetics/electrophysiology, including viral injection, optical fiber implantation, and microelectrode implantation.

To understand how information is processed in neural networks, it is necessary to monitor the activities of neurons at high spatiotemporal resolution (Arenkiel et al., 2007; Anikeeva et al., 2012; Buzsáki et al., 2015; Cardin et al., 2010). Implantable neural probes that transduce extracellular ionic currents into electrical signals are the most widely applied tool to record neural activities at single-cell and sub-millisecond resolution (Hong and Lieber, 2019; Steinmetz et al., 2020). Bioelectrical pulses of individual neurons can be detected by implanted microelectrodes as extracellular action potentials (APs), whereas the collective transmembrane currents from multiple neurons can be detected as local field potentials (LFPs). Combining multi-channel electrical recording with optogenetics can allow for simultaneous recording and modulation of specific types of neurons in target brain regions, which is essential to establish their functions in information processing and animal behavior (Chen et al., 2017; Jeong et al., 2015).

Over the past years, combined optogenetics/electrophysiology techniques have been demonstrated as a powerful tool to dissect the causal relationships between neural activities and behavior outputs. However, there remains a series of challenges in current combined optogenetics/electrophysiology techniques, including limited spatial resolution and tissue damages. This review provides an overview of recent developments in multimodal neural probes for simultaneous optogenetic modulation and electrical recording. We first identify the challenges associated with current combined optogenetics/electrophysiology techniques. Next, we focus on materials and integration strategies of multimodal neural probes for combined optogenetics/electrophysiology with high spatiotemporal precision and low invasiveness. In addition, we also discuss the opportunities of multimodal neural interfaces in basic and translational neuroscience.

## COMBINED OPTOGENETICS/ELECTROPHYSIOLOGY TECHNIQUES

### Challenges in combined optogenetics/electrophysiology techniques

Current combined optogenetics/electrophysiology techniques mainly consist of (1) viral delivery for the expression of light-sensitive opsins in specific types of cells, (2) optical fiber implantation for neural stimulation, and (3) microelectrode implantation for extracellular recording (Figure 1). The virus injection and optical fiber/microelectrode implantation were usually carried out through two separate surgeries (Arenkiel et al., 2007; Cardin et al., 2010; Zhang et al., 2010). A virus vector solution is firstly delivered to a targeted brain region, mostly through stereotaxic injection, to express light-sensitive opsins in specific types of cells. Then a second surgery is carried out to implant an optrode device, consisting of an optical fiber and microelectrodes, into the same region for neural stimulation and recording (Zhang et al., 2010). Although combined optogenetics/electrophysiology techniques have been demonstrated as a powerful tool for dissecting the causal roles of different neural subtypes in neural circuit functions, there still remains a series of technical challenges that need to be solved in order to fully exploit their potentials. For example, visible-light illumination from a

**Table 1. Multimodal neural probes for combined optogenetics and electrophysiology**

Ref	Light source	Probe material	Dimensions	No. of stimulation & recording sites	Benefits	Integration process
Stark et al. (2012) Royer et al. (2012)	Diode-optical fiber assembly; Laser: 470, 589, 639 nm; 561 nm	Silicon/Optical fiber	Diameter: 60–70 $\mu\text{m}$	Sti: 6; 8 Rec: 10 $\times$ 6; 8 $\times$ 8	Large spatial coverage	Manual assembly
Wu et al. (2015)	$\mu\text{LEDs}$ ; Laser: 460 nm	Silicon	Thickness: 30 $\mu\text{m}$ ; Width: 70 $\mu\text{m}$ ; $\mu\text{LED}$ : 11 $\times$ 13 $\mu\text{m}^2$	Sti: 3 $\times$ 4 Rec: 8 $\times$ 4	High spatial precision High density	Microfabrication
Kim et al. (2013)	$\mu\text{LEDs}$ ; Laser: 450 nm	Polymer	Thickness: 20 $\mu\text{m}$ ; Width: 400 $\mu\text{m}$ ; $\mu\text{LED}$ : 50 $\times$ 50 $\mu\text{m}^2$	Sti: 4 Rec: 8	Tetherless Flexibility Long-term stability	Microfabrication
Lin et al. (2017); Lin et al. (2018)	UCNP; Laser: 980 nm	Tungsten wire	Diameter: $\sim$ 80 $\mu\text{m}$	Sti: 1 Rec: 1	Tetherless Remote light source	Manual assembly
Canales et al. (2015); Park et al. (2017)	Polymer; Laser: 473 nm	Polymer	Diameter: $\sim$ 85 $\mu\text{m}$	Sti: 1 Rec: 1	High throughput Flexibility Long-term stability	TDP
Jiang et al. (2020)	Polymer; Laser: 473 nm	Polymer	Diameter: $\sim$ 250 $\mu\text{m}$	Sti: 1 Rec: 5, 7	High throughput Large spatial coverage	TDP
Zou et al. (2021)	Optical fiber; Laser: 473, 589 nm	Polymer	Diameter: $\sim$ 80–220 $\mu\text{m}$	Sti: 1 Rec: 33	High spatial precision Flexibility Long-term stability	Elastocapillary self-assembly

conventional optical fiber usually spreads over hundreds of micrometers to 1 millimeter in the brain (Anikeeva et al., 2012; Pisanello et al., 2017; Royer et al., 2010), which can cause undesirable modulation of neighboring brain regions. The large illumination volume also makes it difficult to separate directly activated neurons from population-mediated neurons (Buzsáki et al., 2015; Royer et al., 2010). In addition, the large sizes and mechanical stiffness of conventional optical fibers and recording microelectrode devices can cause chronic immune reactions and neuronal cell loss around implanted optrodes, limiting their applications in chronic studies. It is thus highly desirable to develop multimodal neural interfaces with high spatial precision and low invasiveness. Recently, a series of important progress have been made in developing multimodal neural interfaces to address these challenges, which we discuss later (Table 1).

### High spatial-resolution optogenetics and electrophysiology

Conventional optrodes are usually manually assembled from optical fibers and microelectrode devices, such as tetrodes or silicon probes. The diameter of a conventional optical fiber is around 200  $\mu\text{m}$ . During optogenetic stimulation, visible light is emitted from the optical fiber in a conical pattern, then scattered and absorbed as it passes through the optically inhomogeneous brain tissue. Previous studies have shown that illumination from a conventional optical fiber can activate or inhibit opsin-expressing neurons within a distance of several hundreds of micrometers to 1 mm (Anikeeva et al., 2012; Airan et al., 2009; Li et al., 2019). On the other hand, microelectrodes can only record from neurons within  $\sim$ 60  $\mu\text{m}$  because extracellular action potential signals decrease exponentially with the distance from neurons (Buzsáki, 2004). As a result, the sizes of optogenetically modulated neuronal populations are typically orders of magnitude larger than that can be electrically recorded, rendering difficulty in assigning the functional roles of the recorded neurons (Buzsáki et al., 2015; Royer et al., 2010). Moreover, high light intensity used in conventional optogenetic modulation can generate superposition of multiple spike waveforms and considerable light artifacts in recorded electrical signals (Kozai and Vazquez, 2015).

To control light illumination volumes during optogenetic modulation, Stark et al. thinned 200- $\mu\text{m}$ -diameter optical fibers down to a diameter of 60–70  $\mu\text{m}$  and sharpened their tips through chemical etching (Figure 2A) (Stark

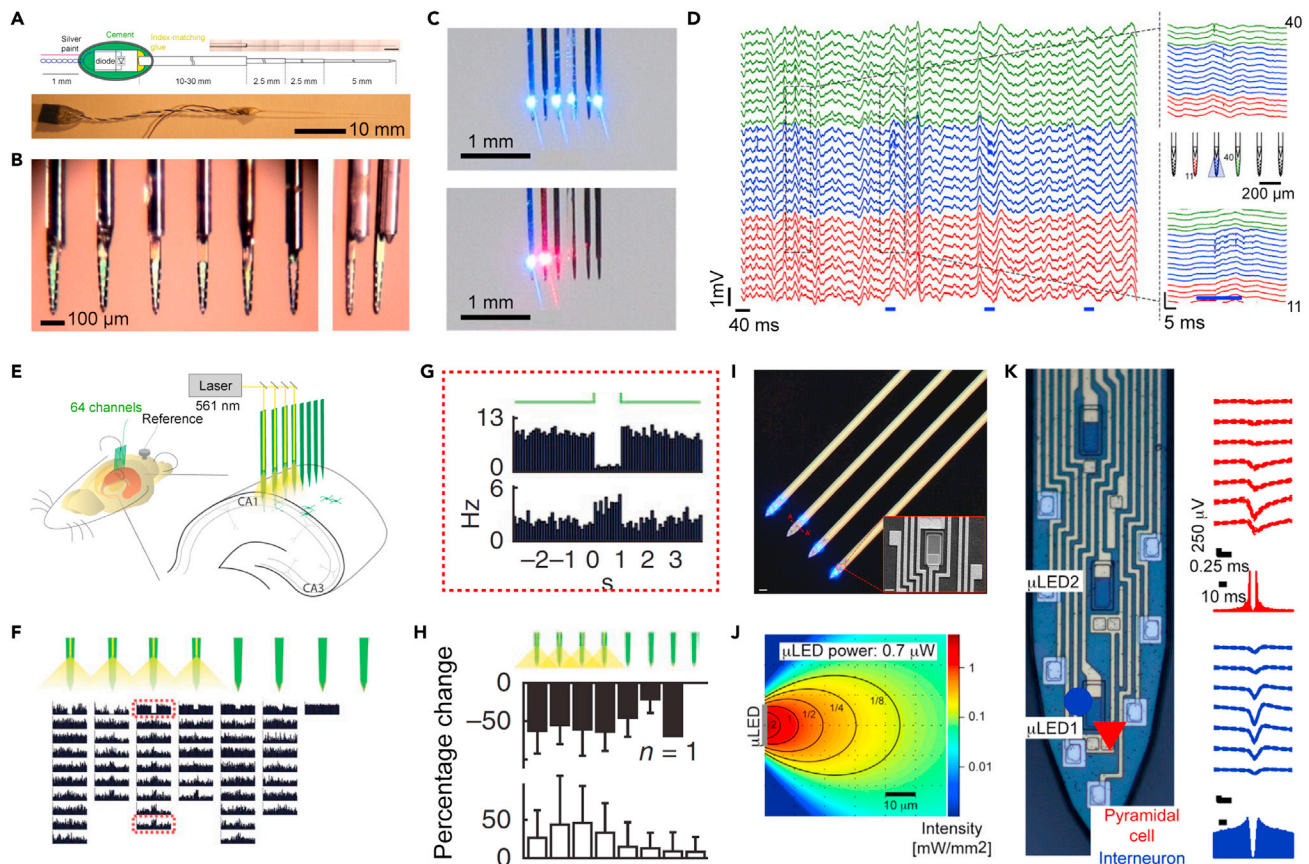


**Figure 2. Multimodal neural probes for high spatiotemporal optogenetics and electrophysiology**

(A) Schematic and picture of a diode-optical fiber assembly.

(B) Optical images of a fiber-probe array. Each fiber-probe array consists of 6 diode-fiber assemblies attached to separate shanks of a six-shank silicon probe. The optical fibers can be separately controlled for localized delivery of light.

(C) Controlled light illumination by fiber-probe arrays. Four shanks in the top panel are used to deliver blue light, and two shanks in the bottom panel are used to deliver blue and red light.

(D) Spatially localized light delivery and neural activation by a fiber-probe array. Panels A to D are reproduced from Stark et al. (2012).

(E) Schematic of simultaneous stimulation and recording of single-unit activity in the hippocampus. Four shanks of an eight-shank silicon probe were attached with diode-fiber assemblies.

(F) Peristimulus histograms of neuronal responses to light pulses that aligned to their respective recording shanks in panel E.

(G) Magnified views of the red dashed boxes in panel F.

(H) Percentage of cells (black, 69 PV cells and white, 722 non-PV cells) with decreased and increased firing rates for each shank. Panels E to H are reproduced from Royer et al. (2012).

(I)  $\mu$ LED-based multifunctional probe. Each shank of the probe is integrated with three interspersed  $\mu$ LEDs and eight Ti/Ir recording sites. Inset is the SEM image of the probe. Scale bars, 70  $\mu$ m and 6  $\mu$ m (inset).

(J) Estimated light output and attenuation when propagating through the brain ambient.

(K) Spiking of a typical pyramidal cell (red triangle) and interneuron (blue circle) during illumination. Panels G to K are reproduced from Wu et al. (2015).

et al., 2012). Each thin optical fiber was then integrated with a light-emitting diode (LED) for localized light delivery and photostimulation (Figures 2B and 2C). For combined optogenetics/electrophysiology, each diode-fiber assembly was attached to a silicon probe with a gap of only 30–40  $\mu$ m. Owing to the small gap between the optical fiber and the recording sites on the silicon probe, a small amount of light (<200  $\mu$ m) from the optical fiber could cover the entire range of the recording sites. Low light intensity also effectively prevented optical artifacts and spike superposition in the recorded electrical signals. To enable multisite optogenetic stimulation and neuronal recordings, they further constructed an optoelectronic array by attaching multiple diode-fiber assemblies to multishank silicon probes (Figure 2D). Each diode could be controlled separately, allowing for localized light stimulation and recording of the stimulated neurons. As an application example, the optoelectronic array was used to focally silence either parvalbumin (PV)- or somatostatin (SOM)-expressing interneurons during

simultaneous recording of place cell activities in hippocampal area CA1 (Figures 2E–2H) (Royer et al., 2012). They found that perisomatic and dendritic inhibition have distinct roles in controlling the rate, burst, and timing of hippocampal pyramidal cells (Shin et al., 2017; Wu et al., 2013; Zorzos et al., 2010).

To achieve high-precision and large-scale optogenetic modulation, microscopic light emitting diodes ( $\mu$ LEDs) can be used to replace optical fibers as implantable light sources (Kim et al., 2013, 2020a; Scharf et al., 2016; Schwaerzle et al., 2013; Wu et al., 2015). For example, Wu et al. monolithically integrated GaN-based  $\mu$ LEDs and recording microelectrodes, with less than twenty micrometers of distance in between, onto silicon probes using microfabrication techniques (Wu et al., 2015). Each  $\mu$ LED and recording microelectrode had dimensions similar to a pyramidal neuron soma (Figures 2I and 2J). The  $\mu$ LED provided tunable illumination power, thus the tissue volume receiving sufficient power to activate ChR2 could be tuned to match the tissue volume within the recording range of its surrounding microelectrodes (Figures 2K). Owing to the close distance between the  $\mu$ LED and its surrounding microelectrodes, light illumination at 60 nW could robustly induce spiking signals, whereas light illumination at the microwatt range could induce fast population oscillations. To demonstrate the scalability of the method, they fabricated a four-shank probe, with each shank consisting of 12  $\mu$ LEDs and 32 recording microelectrodes. The four-shank probe was implanted into the CA1 pyramidal layer in both anesthetized and freely moving mice for simultaneous optogenetic stimulation and electrical recording. Notably, the spatial congruence between optogenetically modulated and electrically recorded neuronal populations, combined with the miniaturized sizes of the optoelectronic components, allowed for cellular-level circuit analysis in freely moving mice. Recently, Kim et al. further extended the capability of the monolithically integrated optoelectrode device for large-scale, high-precision optogenetics and electrophysiology. The device was named HectoSTAR because it could provide optical stimulation to more than one hundred stimulation sites located amid more than 250 recording microelectrodes. HectoSTAR represents one of the most advanced tools for the analysis of wide-ranging, high-density neural circuits at the anatomical resolution (Kim et al., 2020b).

### Multimodal probes for low invasive neural modulation and recording

Low invasive neural modulation and recordings offer important opportunities for both basic and applied neurosciences, including the diagnosis and treatment of neurological diseases. However, previous studies have shown that rigid silicon probes or tetrode probes can cause chronic immune reactions and neuronal cell loss around them. As a result, the recorded electrical signal by a rigid probe usually degrades within a few weeks after implantation (Biran et al., 2005; Kozai et al., 2015). The Young's modulus of a silicon- or metal-based rigid probe is in the range of tens to hundreds of gigapascal (GPa), which is several orders of magnitude higher than that of soft brain tissue (kPa). The large mechanical mismatch between a rigid probe and neural tissue can cause probe-tissue micromotion during pulsation and movement. The magnitude of probe-tissue micromotion is usually in the range of tens to hundreds of micrometers in rodents and can be 1–2 orders of magnitude larger in primates. Over the short term, probe-tissue micromotion results in recording instability because the extracellular signals decay rapidly with the distance from neurons. Over the long term, micromotion-induced shear stress can cause persistent inflammatory responses and glial scar formation around the rigid probe. Glial scar eventually encapsulates the recording microelectrodes as an insulation layer, leading to signal degradation or even loss (Kozai et al., 2015). In optogenetics, the high stiffness and large size of conventional light-delivering optical fibers can also cause acute tissue damages and chronic immune reactions. In addition, fiber tethering can restrict and alter animal behavior. It is thus highly desirable to develop compliant and biocompatible multimodal probes for stable neural interfacing in freely moving animals (Li et al., 2020; Lago and Cester, 2017; Park et al., 2019).

Recently, multifunctional probes based on flexible and biocompatible polymer materials, such as parylene-C, polyimide, and SU-8 (Fu et al., 2017; Guan et al., 2019; He et al., 2020; Jr et al., 2017; Kim et al., 2010; McCall et al., 2013; Tien et al., 2013), have been developed to alleviate micromotion and chronic tissue responses. For example, Kim et al. developed a multifunctional optoelectronic device by integrating  $\mu$ LEDs, recording microelectrodes, and temperature sensors on a polyimide substrate (Figure 3A) (Kim et al., 2013). The multifunctional optoelectronic device has a total thickness of  $\sim 20$   $\mu$ m, resulting in greatly improved flexibility compared with rigid probes (Figures 3B and 3C). A critical challenge for *in vivo* applications of flexible probes is that their high flexibility precludes their direct penetration into deep brain tissue. To address this problem, each optoelectronic device was bonded to a microneedle with a thin and bio-resorbable adhesive silk fibroin (Figure 3D). After implantation into the locus coeruleus (LC) region or ventral

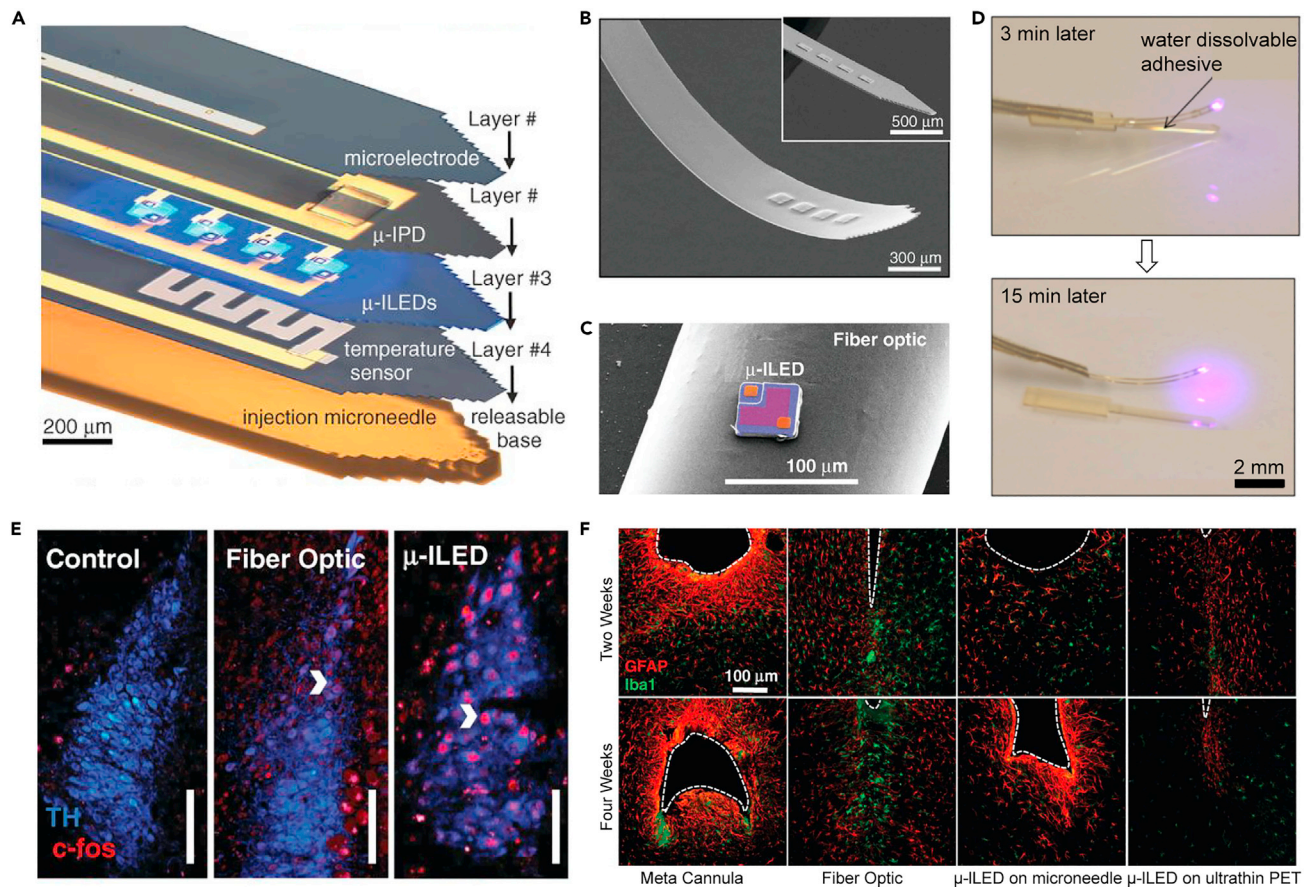


**Figure 3. Flexible multimodal neural probes for minimally invasive optogenetics and electrophysiology**

(A) A multifunctional, implantable optoelectronic device that integrates  $\mu$ -LEDs, microelectrodes, and temperature sensors for optogenetic stimulation, electrophysiological measurement, and temperature sensing.

(B) SEM images of a cellular, injectable optoelectronic device with a total thickness of 8.5  $\mu$ m. Inset figure shows the device before coating with a passivation layer.

(C) The relative size between a  $\mu$ -ILED and 200- $\mu$ m fiber optic implant.

(D) Silk as a water-soluble, bio-resorbable, releasable adhesive for depth implantation of flexible optoelectronic device. The flexible optoelectronic device can be released from the stiff microneedle after the dissolution of silk.

(E) C-fos staining of control (left), fiber-optic-implanted (center), and  $\mu$ -ILED-device-implanted (right) animals. Scale bars, 100  $\mu$ m.

(F) Immunohistochemical staining images of astrocytes (glial fibrillary acidic protein [GFAP], red) and activated microglia (Iba1, green) at the ventral tip of each implanted device (dashed outline). Panels A to F are reproduced from Kim et al. (2013).

tegmental area (VTA) region of mouse brain, the silk fibroin was dissolved by the cerebrospinal fluid, and the microneedle was then detached from the flexible probe and retracted from the brain. Moreover, the  $\mu$ LEDs on the optoelectronic devices could be wirelessly controlled to effectively activate ChR2-expressing neurons (Figure 3E), making it highly suitable for applications in freely moving animals. In addition, the small size and flexibility of the optoelectronic device caused substantially reduced acute lesion and chronic glial activation compared with metal cannulae and fiber optics (Figure 3F). As a result, the flexible device was well tolerated in freely moving animals with encapsulated sensors and  $\mu$ -LEDs maintaining functions over several months.

In optogenetics, visible light (400–700 nm) has been used to manipulate neuronal activities through light-gated opsins (Boyden et al., 2005; Zhang et al., 2008). However, visible light has limited transmission depth in the brain because of its strong absorption and scattering by the brain tissue. As a result, an optical device, such as optical fiber or  $\mu$ -LED, needs to be implanted into a targeted brain region for the delivery of visible light (Cardin et al., 2010; Zhang et al., 2010), which can cause both acute and chronic tissue damages in the brain. To address this issue, red-shifted, high-photocurrent channelrhodopsins have been

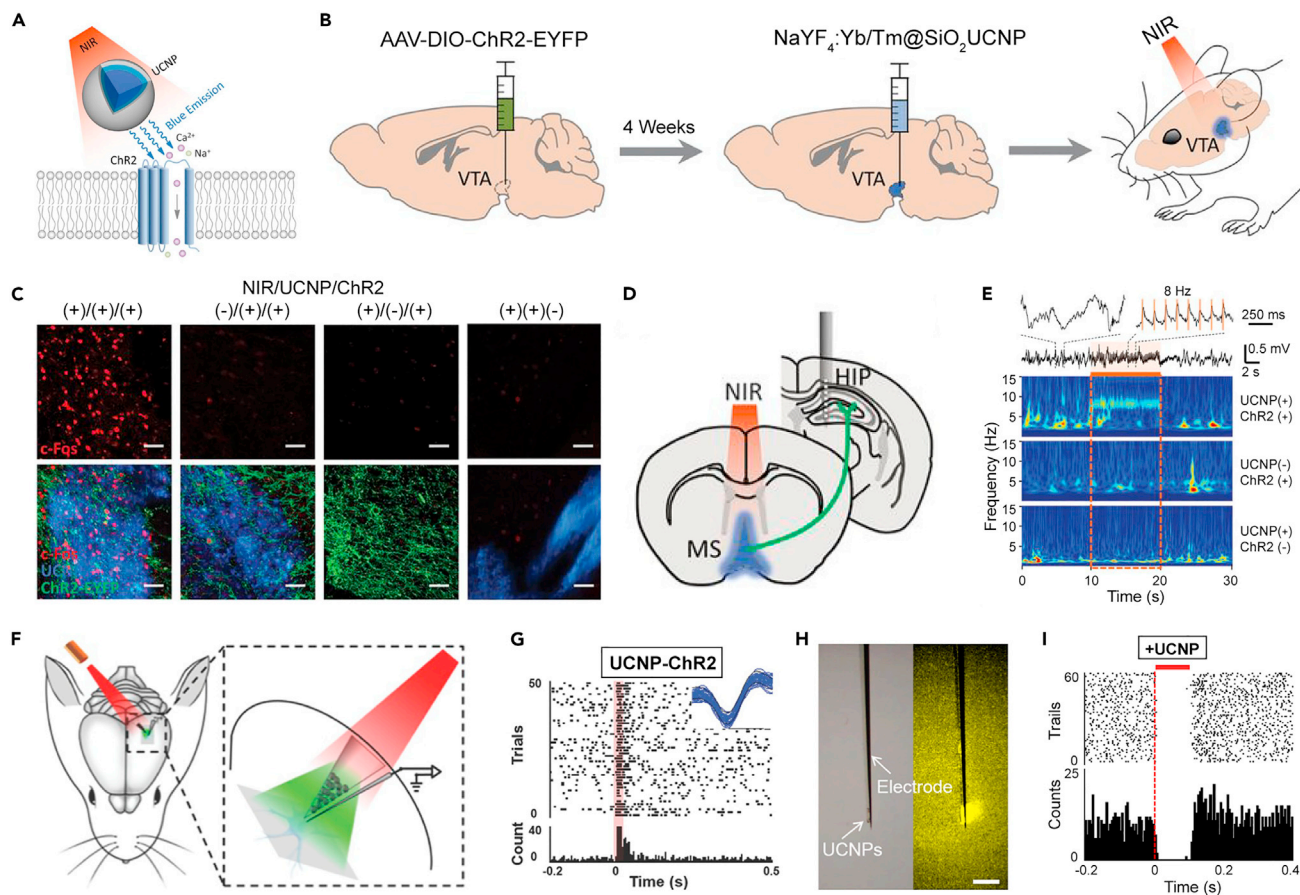


**Figure 4. UCNP-based optogenetics for minimally invasive optogenetics and electrophysiology**

(A) Schematic working principle of UCNP-mediated NIR upconversion optogenetics.

(B) *In vivo* experimental scheme of transcranial NIR stimulation of ventral tegmental area (VTA) in anesthetized mice.

(C) Confocal images of the VTA after transcranial NIR stimulation under different situations. Scale bars, 100  $\mu\text{m}$ .

(D) Illustration of transcranial NIR stimulation of medial septum (MS) for generation of theta oscillations.

(E) Hippocampal LFP in response to transcranial NIR stimulation (8-Hz, 15-ms pulses, 10 s, 3.0-W peak power, 360-mW average power) of MS under different situations. Top: raw LFP trace from mouse with both UCNP and ChR2 injection. Bottom: Z-scored power in the theta range averaged across 30-s trials in all three conditions. Panels A to E are reproduced from [Chen et al. \(2018\)](#).

(F) Schematic of UCNP-mediated simultaneous neural stimulation and extracellular recording in brains of live animals.

(G) Raster plots and peristimulus time histogram that reflects the temporal correlation between increased spiking activity and NIR illumination in ChR2-expressed animals. The inset shows typical spiking waveforms. Panels F to G are reproduced from [Lin et al. \(2017\)](#).

(H) Photograph of a UCNP-based device that without/with 980 nm laser irradiation. Scale bar, 1 mm.

(I) Raster plots and a PSTH (10 ms/bin, 60 trials) showing the temporal correlation between the increased spiking activity and the NIR illumination in eNpHR animals (100 ms pulse width, 6 mW/mm<sup>2</sup>). Panels H to I are reproduced from [Lin et al. \(2018\)](#).

developed by structure-based genome mining. For example, excitatory ChRmine can enable deep brain optogenetics at depths of up to 7 mm with millisecond precision ([Chen et al., 2021](#)). Compared with visible light, near-infrared (NIR) light has greatly reduced absorption and scattering in the brain tissue. Therefore, NIR light can be delivered into deep brain regions (a few millimeters) by placing an optical device above the brain tissue or even through the scalp. Recently, lanthanide-doped upconversion nanoparticles (UCNPs), which can emit wavelength-specific visible light under excitation with NIR light, have attracted significant interests for low invasive neural modulation ([All et al., 2019](#); [Bedbrook et al., 2019](#); [Chen et al., 2018](#); [Hososhima et al., 2015](#); [Lin et al., 2017, 2018](#); [Miyazaki et al., 2019](#); [Zheng et al., 2019](#)). For example, Chen et al. utilized UCNPs as optogenetic actuators of transcranial NIR light to stimulate deep brain neurons in a low invasive manner ([Figure 4A](#)) ([Chen et al., 2018](#)). They incorporated Tm<sup>3+</sup> into Yb<sup>3+</sup>-doped host lattices of UCNPs to achieve blue emission that matches the maximum absorption of channelrhodopsin-2 (ChR2) for neuronal activation. In addition, an optically inert shell layer of NaYF<sub>4</sub> was epitaxially grown

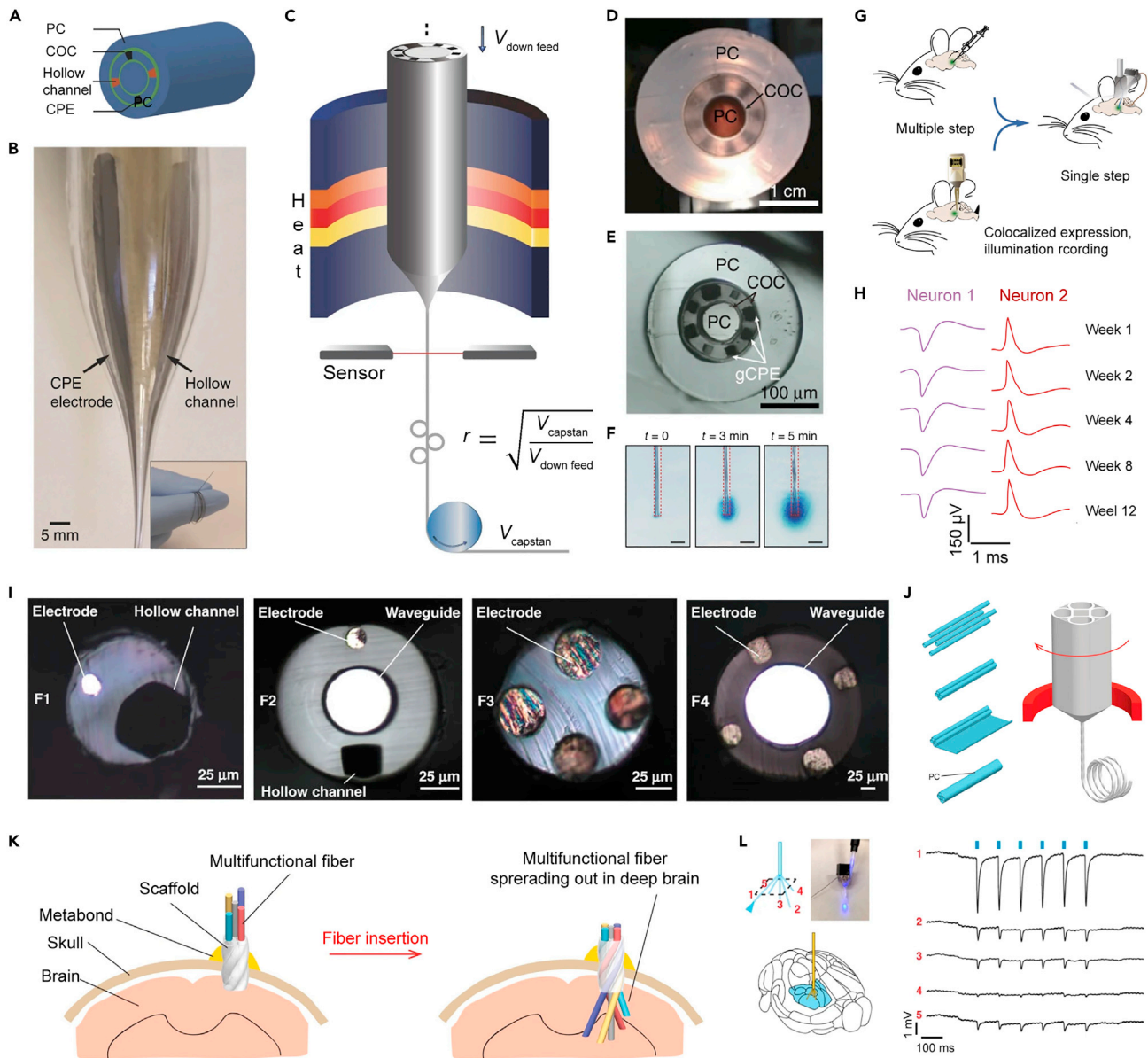


**Figure 5. TDP technology-based multifunctional probes for one-step optogenetics and electrophysiology**

(A) Schematic of a multifunctional fiber preform.

(B) Photograph of the transition part where the design in panel A was drawn into a fiber. Inset shows a photograph showing a multifunctional fiber wrapped around a finger (inset figure). Panels A and B are reproduced from [Canales et al. \(2015\)](#).

(C) Schematic illustration of the thermal drawing process to prepare a multifunctional fiber. The laser sensor was used to monitor the ratio of the capstan and down feed speeds, which determine the diameter of the resulting fiber.

(D) Cross-sectional photograph of a preform before thermal drawing.

(E) Cross-sectional microscope image of a multimodal fiber produced by thermal drawing of the preform in panel E.

(F) Liquid delivery by multimodal fiber. A solution containing Blue Juice dye was injected through a microfluidic channel in a multimodal fiber into a phantom brain (0.6% agarose gel). Scale bar, 500  $\mu\text{m}$ .

(G) Schematic comparison of traditional two-step surgery for optogenetic experiments and one-step surgery using a multifunctional fiber probe.

(H) Average spike waveforms of two mPFC neurons recorded with multifunctional fiber probe over a period of 12 weeks. Panels C to H are reproduced from [Park et al. \(2017\)](#).

(I) A series of fiber-based probes used to prepare spatially expandable probes.

(J) Schematic of the thermal drawing process to prepare spatially expandable probes.

(K) Schematic of the spreading out of the scaffolding fiber after being inserted into the brain.



**Figure 5. Continued**

(L) An illustration of a spatially expanded multimodal fiber probe targeting the thalamus region and a photograph of the assembled device coupled to the 473 nm laser (left), and the electrophysiological recording resulted from 5 electrodes during optogenetic stimulation (right). Panels I to L are reproduced from Jiang et al. (2020).

onto the core (NaYF<sub>4</sub>:Yb/Tm) to eliminate solvent-induced surface quenching of upconversion luminescence. The resulting core-shell UCNPs exhibited a characteristic upconversion emission spectrum peaking at 450 and 475 nm upon excitation at 980 nm. To improve the long-term utility of UCNPs, NaYF<sub>4</sub>:Yb/Tm nanocrystals were further decorated with a biocompatible silica shell (NaYF<sub>4</sub>:Yb/Tm@SiO<sub>2</sub>). An optical fiber (200 μm in diameter) was then placed 2 mm above the skull for the transcranial delivery of 980-nm NIR light (1.4 W/mm<sup>2</sup> NIR on the skull surface) (Figure 4B). Neuronal excitation was triggered by NIR light in ChR2-transfected mice in the presence of UCNPs, as indicated by the significantly higher proportion of c-Fos-positive cells in areas where UCNP injection and ChR2 expression overlapped (Figure 4C). An advantage of UCNP actuators is that their emitted wavelength can be molecularly tailored. To match the maximum absorption of rhodopsins that hyperpolarize neurons, such as NpHR and Arch, the emission of UCNPs was tuned to ~540 nm by codoping Er<sup>3+</sup> and Yb<sup>3+</sup> into the host lattice. Green-emitting UCNPs were utilized to silence seizure by inhibition of hippocampal excitatory cells (Figures 4D and 4E).

The low diffusion capability of UCNPs in the brain tissue makes it extremely challenging to co-localize UCNPs with implanted recording microelectrodes, thus limiting their applications in combined optogenetics/electrophysiology. To address this issue, Lin et al. constructed a UCNP-based multimodal neural probe (Lin et al., 2017, 2018). A series of core-shell- and core-shell-shell-structured UCNPs were prepared to emit visible light for the activation of channelrhodopsin (ChR) and C1V1 or suppression of halorhodopsin (eNpHR) under NIR illumination. The UCNPs were packaged into a sealed glass probe. The glass probe was then integrated with tungsten wires to construct an optrode (Figures 4F and 4G) (Lin et al., 2017). The UCNP-based optrode enabled both the activation of ChR2-expressing neurons and the inhibition of halorhodopsin-expressing neurons upon transcranial NIR light (980 nm) illumination (Figures 4H and 4I) (Lin et al., 2018). However, the footprint and flexibility of the UCNP-based optrode were limited by both the glass probe and tungsten wires, thus limiting their applications in long-term stable neural interfacing.

**One-step optogenetics and electrophysiology**

In conventional optogenetic operation, the virus injection and optrode implantation were usually carried out by two separate surgeries (Anikeeva et al., 2012; Cardin et al., 2010; Zhang et al., 2010). In the first surgery, the virus vector carrying opsin genes was delivered into a targeted brain region. Then a second surgery was carried out to implant an optrode probe into the same region for neural stimulation and recording (Zhang et al., 2010). However, such two-step surgery causes additional tissue damage and is also susceptible to misalignment errors between the optrode implantation site and viral solution injection site. It is thus desirable to integrate gene delivery, optical illumination, and electrical recording in a single platform (Gutruf and Rogers, 2018; Qazi et al., 2019).

Compared with conventional injection methods, microfluidic channels can allow for the delivery of chemical or biological reagents into targeted brain regions in a low invasive manner (Jeong et al., 2015; Madisen et al., 2010; McCall et al., 2017; Spieth et al., 2012; Sim et al., 2017). Microfluidic channels have been integrated with electronic or optoelectronic devices through micro-electro mechanical systems (MEMS) fabrication to construct multifunctional neural probes (Altuna et al., 2013; Canales et al., 2015; Noh et al., 2018; Shin et al., 2015; Zhang et al., 2019). Recently, thermal drawing process (TDP) has emerged as a simple approach to integrate multiple functional units, including microfluidic channels, within a multifunctional fiber with a diameter of a few hundred micrometers and elastic modulus ranging from megapascals to a few gigapascals (Abouraddy et al., 2007; LeChasseur et al., 2011; Park et al., 2017; Tao et al., 2015; Yaman et al., 2011). During the TDP, a preform consisting of optical waveguides, microfluidic channels, and electrodes is thermally annealed and drawn, leading to up to 1–2 orders of magnitude reduction in diameter. By carefully adjusting TDP parameters and materials, the diameter of the multifunctional fiber can be reduced down to a few hundred micrometers while maintaining the macroscopic cross-sectional geometry of the preform. In a pioneer work, Canales et al. developed an innovative multifunctional fiber for simultaneous optical stimulation, neural recording, and drug delivery (Canales et al., 2015). The multifunctional fiber consisted of polymers commonly used in medical devices [poly(etherimide) (PEI), poly(phenylsulfone) (PPSU), polycarbonate (PC), and cyclic olefin copolymer (COC)], a polymer composite (conductive polyethylene (CPE)) and a low-melting-temperature metal (tin (Sn) (Figures 5A–5C). Compared with conventional

microwires, the multifunctional fiber yielded reduced foreign body response and blood-brain barrier (BBB) breaching after implantation. Park et al. developed a multifunctional fiber consisting of an optical waveguide, six electrodes, and two microfluidic channels for one-step optogenetics (Park et al., 2017). The multifunctional fiber was fabricated solely from polymers and polymer composites and had a total diameter of less than 200  $\mu\text{m}$ . To improve electrode conductivity, conductive polyethylene (CPE) was mixed with 5% in weight of graphite, resulting in a 4.1-fold reduction of the sheet resistance of the polymer composite (Figures 5D–5F). Their probes allowed for one-step surgery including microfluidic delivery of viral vectors carrying opsin genes into specific locations of the mouse brain and subsequent optical stimulation and recording of neural activity (Figure 5G). Robust Chr2 expression was observed 2 weeks after microfluidic injection of an adeno-associated virus (AAV) solution in the medial prefrontal cortex of wild-type mice. In addition, the flexibility and miniaturized footprint of the multifunctional fiber enhanced its biocompatibility in mouse brain, enabling long-term recordings of single neurons for over 3 months (Figure 5H).

To achieve synchronous recording and modulation of brain activities across multiple brain regions, Jiang et al. fabricated a spatially expandable multifunctional fiber probe by TDP technique (Jiang et al., 2020). Multifunctional fibers, consisting of an optical waveguide, microfluidic channels, and BiSn metal alloy electrodes, were firstly fabricated using the TDP process (Figure 5I). Next, a femtosecond laser micromachining technique was applied to expose multiple optical, electrical, and microfluidic interfacing sites along the multifunctional fiber. Lastly, a helical scaffolding fiber was developed for producing spatially expandable fiber probes (Figure 5J). PC tubes were bundled and wrapped with a thin layer of PC to form a preform with four round holes and one square hole. The preform was then drawn into a scaffolding fiber with helix hollow channels by using a customized preform feeding stage that could allow simultaneous translation and rotation of the preform. For *in vivo* applications, an array of multifunctional fibers was inserted into the hollow channels of a helical scaffolding fiber. The helical scaffolding fiber could direct multifunctional fiber probes into the brain tissue at specified angles, allowing for the three-dimensional spatial expansion of the multifunctional fiber probes (Figure 5K). The spatially expandable multifunctional fiber-based probes were further demonstrated for mapping and modulating brain activities across distant regions in Thy1-ChR2-YFP mice (Figure 5L).

Polymer represents one of the most widely applied carrier platforms for efficient encapsulation and delivery of drugs and genes in biomedical applications. To achieve targeted delivery of AAV vectors expressing opsin proteins, Jackman et al. developed a one-step optogenetics technique by coating optical fibers or endoscopes with films composed of silk fibroin and AAV (Jackman et al., 2018). Silk fibroin was chosen as the AAV carrier because of its biocompatibility, controllable degradability, and water solubility (Fernández-García et al., 2016; Kim et al., 2010; Raja et al., 2013; Yin et al., 2018). After implantation, silk fibroin was dissolved by cerebrospinal fluid, and virus vectors were released to transduce nearby cells for localized opsin expression around optical fibers and endoscopes (Figures 6A–6C). Recently, Zou et al. developed a self-assembled viral vector delivering (VVD) optrode for precise integration of optogenetics and electrophysiology (Zou et al., 2021). An array of ultraflexible microelectrode filaments (MEFs) and optical fiber were immersed in a viral vector containing PEG melt and then withdrawn into ambient air. Driven by elastocapillary interactions, the MEFs and optical fiber self-assembled into a thin and stiff VVD optrode (Figures 6D and 6E). After implantation in the brain, the dissolution of the PEG carrier allows highly localized viral delivery and neuronal expression of opsin genes within a distance of  $\sim 100\ \mu\text{m}$  from ultraflexible microelectrodes (Figures 6F). The highly localized transfection of opsin proteins ensured high spatial congruence between optogenetically manipulated and recorded neuronal populations. Owing to the high flexibility of the MEFs, chronically implanted VVD-delivery optrode enabled long-term optogenetic activation/inhibition and electrical recordings of neuronal activities in the brain (Figures 6G and 6H). A wide variety of AAV, biomolecules, or therapeutic agents could be embedded into the nanoliter-scale PEG carrier of this system for spatially confined drug/gene delivery and modulation of cellular functions at microelectrode-tissue interfaces. Thus this development might pave the way toward a versatile platform for high-precision neural circuit analysis and engineering in basic and translational neuroscience.

## CONCLUSION AND OUTLOOK

Advances in neuroscience have been driven by the development of neural modulation and recording technologies. Multimodal neural probes that combine optogenetics with electrophysiology can allow for simultaneous modulation and recording of specific types of neurons in target brain regions, representing a powerful tool for the dissection of neural circuit functions. Over the past decade, multimodal neural probes have allowed for simultaneous neural recording and stimulation with high spatiotemporal precision and

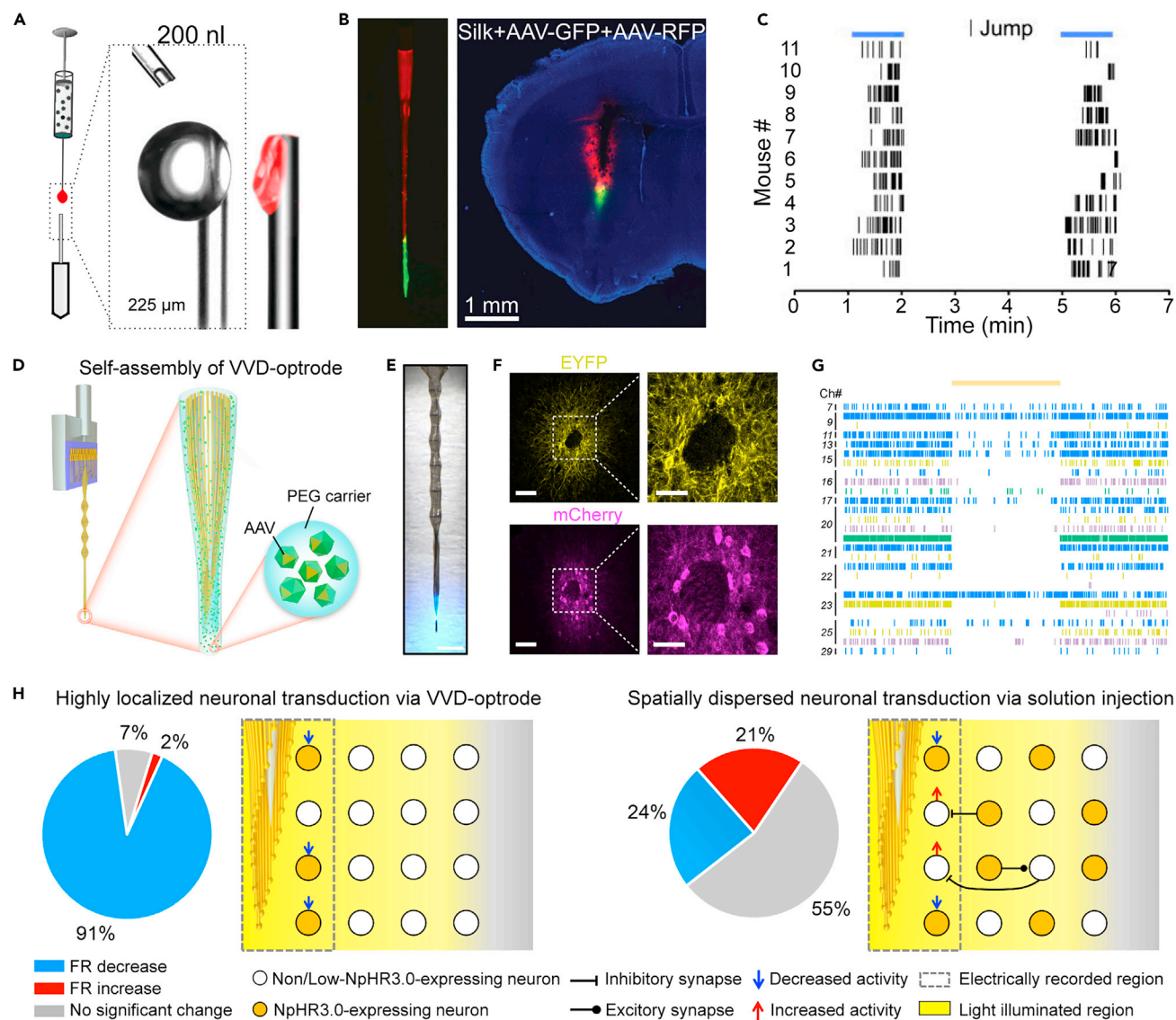


**Figure 6. Examples of multimodal optrodes integrate simultaneous optical, electrical, and gene delivery**

(A) Schematic of the preparation of silk/AAV-loaded implants.  
 (B) Silk/AAV-loaded implant containing green dye on the tip and red dye up the shaft (left) for the expression of both RFP and GFP (right).  
 (C) Raster plot of jumps elicited by optical stimulation in 11 animals. Panels A to C are reproduced from [Jackman et al. \(2018\)](#).  
 (D) Schematic of an elastocapillary self-assembled VVD-optrode for simultaneous AAV vector delivery, neural signal recording, and light stimulation.  
 (E) A VVD-optrode with light on. Scale bar, 1 mm.  
 (F) Spatially localized eNpHR:YFP and Chr2:mCherry expression around implanted VVD-delivery probe. Scale bars, 100  $\mu\text{m}$  and 50  $\mu\text{m}$  (magnified views).  
 (G) Spike rasters of 27 neurons during yellow light stimulation.  
 (H) Percentage of neurons with a decrease or an increase in firing rates during yellow light (589 nm) stimulation. Panels D to H are reproduced from [Zou et al. \(2021\)](#).

biocompatibility. In addition, significant progress has been made in translational application of combined optogenetics/electrophysiology techniques. For example, closed-loop BCIs based on combined optogenetics/electrophysiology can record neural activity and process it in real time for optogenetic stimulation of neural activity and has shown great promise for seizure control and peripheral neuromodulation ([Grosenick et al., 2015](#); [Kuo et al., 2018](#); [Mickle et al., 2019](#); [Zhang et al., 2021](#)). Wireless implantable devices have enabled long-lasting and high-fidelity interfaces for electrical recording and optogenetic stimulation in free-moving animals ([Gutruf and Rogers., 2018](#); [Jeong et al., 2015](#); [McCall et al., 2013, 2017](#); [Noh et al., 2018](#); [Qazi et al., 2019](#); [Shin et al., 2017](#); [Zhang et al., 2019](#)).

Despite substantial progress in the development of multimodal tools for combined optogenetics and electrophysiology, many challenges remain to be addressed. For example, microLED-integrated multimodal probes can allow for spatially precise delivery of low-intensity light at microelectrode-tissue interfaces, constituting a promising tool for high-density dissection of neural circuit functions (Buzsáki et al., 2015; Wu et al., 2015). However, current high-density microLED-integrated multimodal probes have been mainly fabricated on silicon substrates, and the rigidity of these probes can cause chronic tissue responses and limit their long-term applications. UCNP can convert transcranial NIR light to visible light in deep brain tissues, allowing for fiberless optogenetics (Chen et al., 2018; Miyazaki et al., 2019). In addition, injectable photoreceptor-binding UCNP nanoparticles have been shown to enable mice to develop infrared vision, making them a promising candidate for visual repair and enhancement (Ma et al., 2019). However, current UCNP materials are limited by low efficiency in NIR-to-visible conversion (Zheng et al., 2019). As a result, high-intensity NIR light is needed to control the activity of opsin-expressing neurons, which, however, can result in overheating and tissue damages. In addition, the long-term biocompatibility of UCNP and other nanomaterial-based neuromodulators remains to be established before their biomedical applications. Thermally drawn multifunctional fibers can allow for combined optogenetics/electrophysiology via one-step surgery (Canales et al., 2015; Park et al., 2017). However, thermally drawn multifunctional fibers currently consist of only a small number of recording sites, thus limiting their applications in high-density neural interfacing. Nevertheless, the versatility in the design of thermally drawn multifunctional fibers, combined with their high-throughput production, makes them a promising candidate for interfacing neural systems and treating various neurological diseases.

Simultaneous modulation and recording of a large number of neurons over multiple timescales represents one of the ultimate goals in basic and translational neuroscience. To achieve this goal, it is highly desirable to develop multimodal neural probes with high-density integrated modulation and recording sites. Although considerable progress has been made over the past years, it is still challenging to overcome the conflicts between the requirements to increase the modulation and recording site numbers and the demands to minimize the integrated footprints and related tissue damages in multimodal neural probes (Chung et al., 2019). In addition, it is also desirable for multimodal neural probes to cover multiple areas and depths in the brain to study the emerging functional connectivity of neural circuits (Xie et al., 2015). Thus, we foresee that a frontier of research in multimodal neural probes will be to minimize the sizes of modulation and recording sites down to cellular and even subcellular dimensions and to integrate these components on soft, biocompatible substrate materials in high-density and large-scale manner.

Future research topics also include further expansion of the sensing modalities of multimodal neural probes, including temperature, pH, and neurotransmitters. In addition, optofluidic neural probes that combine microfluidic drug delivery with cellular-scale inorganic light-emitting diode arrays have been demonstrated in freely moving animals to modify gene expression, deliver peptide ligands, and manipulate animal behavior. Integrating these capabilities in combined optogenetics and electrophysiology, especially in a wireless manner (Jeong et al., 2015; Qazi et al., 2019; McCall et al., 2017; Noh et al., 2018), holds great promise in the diagnosis and treatment of neurological disorders. To achieve these goals, a coordinated effort from basic research, translational research, and clinical research teams will be required to make these multimodal neural probes widely accessible in basic and clinical neuroscience applications.

## ACKNOWLEDGMENTS

This work is supported by the National Natural Science Foundation of China (Grant nos. 21790393, 21673057, and 22102040) and the Strategic Priority Research Program of the Chinese Academy of Science (Grant no. XDB32030100).

## AUTHOR CONTRIBUTIONS

H.T. performed a literature search and prepared figures. Y.F. provided the guidance and framework of the study. H.T. and Y.F. wrote the manuscript with input from all authors.

## DECLARATION OF INTERESTS

The authors declare no competing interests.

## REFERENCES

- Abouraddy, A.F., Bayindir, M., Benoit, G., Hart, S.D., Kuriki, K., Orf, N., Shapira, O., Sorin, F., Temelkuran, B., and Fink, Y. (2007). Towards multimaterial multifunctional fibres that see, hear, sense and communicate. *Nat. Mater.* 6, 336–347.
- Airau, R.D., Thompson, K.R., Fenno, L.E., Bernstein, H., and Deisseroth, K. (2009). Temporally precise in vivo control of intracellular signalling. *Nature* 458, 1025–1029.
- All, A.H., Zeng, X., Teh, D.B.L., Yi, Z., Prasad, A., Ishizuka, T., Thakor, N., Hiromu, Y., and Liu, X. (2019). Expanding the toolbox of upconversion nanoparticles for in vivo optogenetics and neuromodulation. *Adv. Mater.* 31, 1803474.
- Altuna, A., Bellistri, E., Cid, E., Aivar, P., Gal, B., Berganzo, J., Gabriel, G., Guimerà, A., Villa, R., Fernández, L.J., and de la Prida, L.M. (2013). SU-8 based microprobes for simultaneous neural depth recording and drug delivery in the brain. *Lab. Chip.* 13, 1422–1430.
- Anikeeva, P., Andalman, A.S., Witten, I., Warden, M., Goshen, I., Grosenick, L., Gunaydin, L.A., Frank, L.M., and Deisseroth, K. (2012). Optetrode: a multichannel readout for optogenetic control in freely moving mice. *Nat. Neurosci.* 15, 163–170.
- Arenkiel, B.R., Peca, J., Davison, I.G., Feliciano, C., Deisseroth, K., Augustine, G.J., Ehlers, M.D., and Feng, G. (2007). In vivo light-induced activation of neural circuitry in transgenic mice expressing channelrhodopsin-2. *Neuron* 54, 205–218.
- Bedbrook, C.N., Yang, K.K., Robinson, J.E., Mackey, E.D., Gradinaru, V., and Arnold, F.H. (2019). Machine learning-guided channelrhodopsin engineering enables minimally invasive optogenetics. *Nat. Methods* 16, 1176–1184.
- Biran, R., Martin, D.C., and Tresco, P.A. (2005). Neuronal cell loss accompanies the brain tissue response to chronically implanted silicon microelectrode arrays. *Exp. Neurol.* 195, 115–126.
- Borchers, S., Himmelbach, M., Logothetis, N., and Karnath, H.-O. (2012). Direct electrical stimulation of human cortex - the gold standard for mapping brain functions? *Nat. Rev. Neurosci.* 13, 63–70.
- Boyden, E.S., Zhang, F., Bamberg, E., Nagel, G., and Deisseroth, K. (2005). Millisecond-timescale, genetically targeted optical control of neural activity. *Nat. Neurosci.* 8, 1263–1268.
- Buzsáki, G. (2004). Large-scale recording of neuronal ensembles. *Nat. Neurosci.* 7, 446–451.
- Buzsáki, G., Stark, E., Berényi, A., Khodagholy, D., Kipke, D.R., Yoon, E., and Wise, K.D. (2015). Tools for probing local circuits: high-density silicon probes combined with optogenetics. *Neuron* 86, 92–105.
- Canales, A., Jia, X., Frierip, U.P., Koppes, R.A., Tringides, C.M., Selvidge, J., Lu, C., Hou, C., Wei, L., Fink, Y., et al. (2015). Multifunctional fibers for simultaneous optical, electrical and chemical interrogation of neural circuits in vivo. *Nat. Biotech.* 33, 277–284.
- Cardin, J.A., Carlén, M., Meletis, K., Knoblich, U., Zhang, F., Deisseroth, K., Tsai, L.-H., and Moore, C.I. (2010). Targeted optogenetic stimulation and recording of neurons in vivo using cell-type-specific expression of Channelrhodopsin-2. *Nat. Protoc.* 5, 247–254.
- Chen, R., Canales, A., and Anikeeva, P. (2017). Neural recording and modulation technologies. *Nat. Rev. Mater.* 2, 16093.
- Chen, S., Weitemier, A.Z., Zeng, X., He, L., Wang, X., Tao, Y., Huang, A.J.Y., Hashimoto, Y., Kano, M., Iwasaki, H., et al. (2018). Near-infrared deep brain stimulation via upconversion nanoparticle-mediated optogenetics. *Science* 359, 679–684.
- Chen, R., Gore, F., Nguyen, Q.-A., Ramakrishnan, C., Patel, S., Kim, S.H., Raffiee, M., Kim, Y.S., Hsueh, B., Krook-Magnusson, E., et al. (2021). Deep brain optogenetics without intracranial surgery. *Nat. Biotechnol.* 39, 161–164.
- Chung, J.E., Joo, H.R., Fan, J.L., Liu, D.F., Barnett, A.H., Chen, S., Geaghan-Breiner, C., Karlsson, M.P., Karlsson, M., Lee, K.Y., et al. (2019). High-density, long-lasting, and multi-region electrophysiological recordings using polymer electrode arrays. *Neuron* 101, 21–31.
- Cogan, S.F. (2008). Neural stimulation and recording electrodes. *Annu. Rev. Biomed. Eng.* 10, 275–309.
- Deisseroth, K. (2011). Optogenetics. *Nat. Methods* 8, 26–29.
- Deisseroth, K. (2015). Optogenetics 10 years of microbial opsins in neuroscience. *Nat. Neurosci.* 18, 1213–1225.
- Fernández-García, L., Mari-Buyé, N., Barrios, J.A., Madurga, R., Elices, M., Pérez-Rigueiro, J., Ramos, M., Guinea, G.V., and González-Nieto, D. (2016). Safety and tolerability of silk fibroin hydrogels implanted into the mouse brain. *Acta Biomater.* 45, 262–275.
- Frank, J.A., Antonini, M.-J., and Anikeeva, P. (2019). Next-generation interfaces for studying neural function. *Nat. Biotechnol.* 37, 1013–1023.
- Fu, T.-M., Hong, G., Viveros, R.D., Zhou, T., and Lieber, C.M. (2017). Highly scalable multichannel mesh electronics for stable chronic brain electrophysiology. *Proc. Natl. Acad. Sci. U S A* 114, E10046–E10055.
- Gradinaru, V., Thompson, K.R., and Deisseroth, K. (2008). eNpHR: a natronomonas halorhodopsin enhanced for optogenetic applications. *Brain Cell Biol.* 36, 129–139.
- Gradinaru, V., Mogri, M., Thompson, K.R., Henderson, J.M., and Deisseroth, K. (2009). Optical deconstruction of parkinsonian neural circuitry. *Science* 324, 354–359.
- Grosenick, L., Marshel, J.H., and Deisseroth, K. (2015). Closed-loop and activity-guided optogenetic control. *Neuron* 86, 106–139.
- Guan, S., Wang, J., Gu, X., Zhao, Y., Hou, R., Fan, H., Zou, L., Gao, L., Du, M., Li, C., and Fang, Y. (2019). Elastocapillary self-assembled neurotassels for stable neural activity recordings. *Sci. Adv.* 5, eaav2842.
- Gutruf, P., and Rogers, J.A. (2018). Implantable, wireless device platforms for neuroscience research. *Curr. Opin. Neurobiol.* 50, 42–49.
- Han, X., Qian, X., Bernstein, J.G., Zhou, H., Franzesi, G.T., Stern, P., Bronson, R.T., Graybiel, A.M., Desimone, R., and Boyden, E.S. (2009). Millisecond-timescale optical control of neural dynamics in the nonhuman primate brain. *Neuron* 62, 191–198.
- He, F., Lycke, R., Ganji, M., Xie, C., and Luan, L. (2020). Ultraflexible neural electrodes for long-lasting intracortical recording. *iScience* 23, 101387.
- Herculano-Houzel, S. (2009). The human brain in numbers: a linearly scaled-up primate brain. *Front. Hum. Neurosci.* 3, 31.
- Hong, G., and Lieber, C.M. (2019). Novel electrode technologies for neural recordings. *Nat. Rev. Neurosci.* 20, 330–345.
- Hososhima, S., Yuasa, H., Ishizuka, T., Hoque, M.R., Yamashita, T., Yamanaka, A., Sugano, E., Tomita, H., and Yawo, H. (2015). Near-infrared (NIR) up-conversion optogenetics. *Sci. Rep.* 5, 16533.
- Jackman, S.L., Chen, C.H., Chettih, S.N., Neufeld, S.O., Drew, I.R., Agba, C.K., Flaquer, I., Stefano, A.N., Kennedy, T.J., Belinsky, J.E., et al. (2018). Silk fibroin films facilitate single-step targeted expression of optogenetic proteins. *Cell Rep.* 22, 3351–3361.
- Jeong, J.-W., McCall, J.G., Shin, G., Zhang, Y., Al-Hasani, R., Kim, M., Li, S., Sim, J.Y., Jang, K.-I., Shi, Y., et al. (2015). Wireless optofluidic systems for programmable in vivo pharmacology and optogenetics. *Cell* 162, 662–674.
- Jiang, S., Patel, D.C., Kim, J., Yang, S., Lii, W.A.M., Zhang, Y., Wang, K., Feng, Z., Vijayan, S., Cai, W., et al. (2020). Spatially expandable fiber-based probes as a multifunctional deep brain interface. *Nat. Commun.* 11, 6115.
- Jr, S.T.G., Yao, J., Hong, G., Fu, T.-M., and Lieber, C.M. (2017). Syringe-injectable electronics with a plug-and-play input/output interface. *Nano. Lett.* 17, 5836–5842.
- Kim, D.-H., Viventi, J., Amsden, J., Xiao, J., Vigeland, L., Kim, Y.-S., Blanco, J.A., Panilaitis, B., Frechette, E.S., Contreras, D., et al. (2010). Dissolvable films of silk fibroin for ultrathin conformal bio-integrated electronics. *Nat. Mater.* 9, 511–517.
- Kim, T.-i., McCall, J.G., Jung, Y.H., Huang, X., Siuda, E.R., Li, Y., Song, J., Song, Y.M., Pao, H.A., Kim, R.-H., et al. (2013). Injectable, cellular-scale optoelectronics with applications for wireless optogenetics. *Science* 340, 211–216.
- Kim, C.K., Adhikari, A., and Deisseroth, K. (2017). Integration of optogenetics with complementary methodologies in systems neuroscience. *Nat. Rev. Neurosci.* 18, 222–235.
- Kim, K., Vörös, M., Seymour, J.P., Wise, K.D., Buzsáki, G., and Yoon, E. (2020a). Artifact-free

and high-temporal-resolution in vivo opto-electrophysiology with microLED optoelectrodes. *Nat. Commun.* 11, 2063.

Kim, K., Vöröslako, M., Fernández-Ruiz, A., Parizi, S.S., Ko, E., Hendrix, B., Seymour, J.P., Wise, K.D., Buzsáki, G., and Yoon, E. (2020b). HectoSTAR microLED optoelectrodes for large-scale, high-precision in vivo opto-electrophysiology. *bioRxiv*. <https://doi.org/10.1101/2020.10.09.334227>.

Kohara, K., Pignatelli, M., Rivest, A.J., Jung, H.-Y., Kitamura, T., Suh, J., Frank, D., Kajikawa, K., Mise, N., Obata, Y., et al. (2014). Cell type-specific genetic and optogenetic tools reveal hippocampal CA2 circuits. *Nat. Neurosci.* 17, 269–279.

Kozai, T.D.Y., and Vazquez, A.L. (2015). Photoelectric artifact from optogenetics and imaging on microelectrodes and bioelectronics: new challenges and opportunities. *J. Mater. Chem. B* 3, 4965–4978.

Kozai, T.D.Y., Jaquins-Gerstl, A.S., Vazquez, A.L., Michael, A.C., and Cui, X.T. (2015). Brain tissue responses to neural implants impact signal sensitivity and intervention strategies. *ACS Chem. Neurosci.* 6, 48–67.

Kuo, C.-H., White-Dzuro, G.A., and Ko, A.L. (2018). Approaches to closed-loop deep brain stimulation for movement disorders. *Neurosurg. Focus* 45, E2.

Lago, N., and Cester, A. (2017). Flexible and organic neural interfaces: a Review. *App. Sci.* 7, 1292.

LeChasseur, Y., Dufour, S., Lavertu, G., Bories, C., Deschênes, M., Vallée, R., and Koninck, Y.D. (2011). A microprobe for parallel optical and electrical recordings from single neurons in vivo. *Nat. Methods* 8, 319–325.

Li, N., Chen, S., Guo, Z.V., Chen, H., Huo, Y., Inagaki, H.K., Chen, G., Davis, C., Hansel, D., Guo, C., and Svoboda, K. (2019). Spatiotemporal constraints on optogenetic inactivation in cortical circuits. *eLife* 8, e48622.

Li, H., Wang, J., and Fang, Y. (2020). Bioinspired flexible electronics for seamless neural interfacing and chronic recording. *Nanoscale Adv.* 2, 3095–3102.

Lin, X., Wang, Y., Chen, X., Yang, R., Wang, Z., Feng, J., Wang, H., Lai, K.W.C., He, J., Wang, F., and Shi, P. (2017). Multiplexed optogenetic stimulation of neurons with spectrum-selective upconversion nanoparticles. *Adv. Healthc. Mater.* 6, 1700446.

Lin, X., Chen, X., Zhang, W., Sun, T., Fang, P., Liao, Q., Chen, X., He, J., Liu, M., Wang, F., and Shi, P. (2018). Core-shell-shell upconversion nanoparticles with enhanced emission for wireless optogenetic inhibition. *Nano. Lett.* 18, 948–956.

Ma, Y., Bao, J., Zhang, Y., Li, Z., Zhou, X., Wan, C., Huang, L., Zhao, Y., Han, G., and Xue, T. (2019). Mammalian near-infrared image vision through injectable and self-powered retinal nanoantennae. *Cell* 177, 243–255.

Madisen, L., Zwingman, T.A., Sunkin, S.M., Oh, S.W., Zariwala, H.A., Gu, H., Ng, L.L., Palmiter, R.D., Hawrylycz, M.J., Jones, A.R., et al. (2010). A

robust and high-throughput Cre reporting and characterization system for the whole mouse brain. *Nat. Neurosci.* 13, 133–140.

McCall, J.G., Kim, T.-I., Shin, G., Huang, X., Jung, Y.H., Al-Hasani, R., Omenetto, F.G., Bruchas, M.R., and Rogers, J.A. (2013). Fabrication and application of flexible, multimodal light-emitting devices for wireless optogenetics. *Nat. Protoc.* 8, 2413–2428.

McCall, J.G., Qazi, R., Shin, G., Li, S., Ikram, M.H., Jang, K.-I., Liu, Y., Al-Hasani, R., Bruchas, M.R., Jeong, J.-W., and Rogers, J.A. (2017). Preparation and implementation of optofluidic neural probes for in vivo wireless pharmacology and optogenetics. *Nat. Protoc.* 12, 219–237.

Mickle, A.D., Won, S.M., Noh, K.N., Yoon, J., Meacham, K.W., Xue, Y., McIlvried, L.A., Copits, B.A., Samineni, V.K., Crawford, K.E., et al. (2019). A wireless closed-loop system for optogenetic peripheral neuromodulation. *Nature* 565, 361–365.

Miyazaki, T., Chowdhury, S., Yamashita, T., Matsubara, T., Yawo, H., Yuasa, H., and Yamanaka, A. (2019). Large timescale interrogation of neuronal function by fiberless optogenetics using lanthanide micro-particles. *Cell Rep.* 26, 1033–1043.

Noh, K.N., Park, S.I., Qazi, R., Zou, Z., Mickle, A.D., Grajales-Reyes, J.G., Jang, K.-I., Gereau IV, R.W., Xiao, J., Rogers, J.A., et al. (2018). Miniaturized, battery-free optofluidic systems with potential for wireless pharmacology and optogenetics. *Small* 14, 1702479.

O’Shea, D.J., Kalanithi, P., Ferenczi, E.A., Hsueh, B., Chandrasekaran, C., Goo, W., Diester, I., Ramakrishnan, C., Kaufman, M.T., Ryu, S.I., et al. (2018). Development of an optogenetic toolkit for neural circuit dissection in squirrel monkeys. *Sci. Rep.* 8, 6775.

Paoletti, P., Ellis-Davies, G.C.R., and Mouro, A. (2019). Optical control of neuronal ion channels and receptors. *Nat. Rev. Neurosci.* 20, 514–532.

Park, S., Guo, Y., Jia, X., Choe, H.K., Grena, B., Kang, J., Park, J., Lu, C., Canales, A., Chen, R., et al. (2017). One-step optogenetics with multifunctional flexible polymer fibers. *Nat. Neurosci.* 20, 612–619.

Park, S., Loke, G., Fink, Y., and Anikeeva, P. (2019). Flexible fiber-based optoelectronics for neural interfaces. *Chem. Soc. Rev.* 48, 1826–1852.

Pastrana, E. (2011). Optogenetics: controlling cell function with light. *Nat. Methods* 8, 24–25.

Pisanello, F., Mandelbaum, G., Pisanello, M., Oldenburg, I.A., Sileo, L., Markowitz, J.E., Peterson, R.E., Patria, A.D., Haynes, T.M., Emara, M.S., et al. (2017). Dynamic illumination of spatially restricted or large brain volumes via a single tapered optical fiber. *Nat. Neurosci.* 20, 1180–1188.

Qazi, R., Gomez, A.M., Castro, D.C., Zou, Z., Sim, J.Y., Xiong, Y., Abdo, J., Kim, C.Y., Anderson, A., Lohner, F., et al. (2019). Wireless optofluidic brain probes for chronic neuropharmacology and photostimulation. *Nat. Biomed. Eng.* 3, 655–669.

Raja, W.K., MacCorkle, S., Diwan, I.M., Abdurrob, A., Lu, J., Omenetto, F.G., and Kaplan, D.L.

(2013). Transdermal delivery devices: fabrication, mechanics and drug release from silk. *Small* 9, 3704–3713.

Royer, S., Zemelman, B.V., Barbic, M., Losonczy, A., Buzsáki, G., and Magee, J.C. (2010). Multi-array silicon probes with integrated optical fibers light assisted perturbation and recording of local neural circuits in the behaving animal. *Eur. J. Neurosci.* 31, 2279–2291.

Royer, S., Zemelman, B.V., Losonczy, A., Kim, J., Chance, F., Magee, J., and Buzsáki, G. (2012). Control of timing, rate and bursts of hippocampal place cells by dendritic and somatic inhibition. *Nat. Neurosci.* 15, 769–775.

Scharf, R., Tsunematsu, T., McAlinden, N., Dawson, M.D., Sakata, S., and Mathieson, K. (2016). Depth-specific optogenetic control in vivo with a scalable, high-density  $\mu$ LED neural probe. *Sci. Rep.* 6, 28381.

Shin, H., Lee, H.J., Chae, U., Kim, H., Kim, J., Choi, N., Woo, J., Cho, Y., Lee, J., Yoon, E.-S., et al. (2015). Neural probes with multi-drug delivery capability. *Lab. Chip* 15, 3730–3737.

Schwaerzle, M., Seidl, K., Schwarz, U.T., Paul, O., and Ruther, P. (2013). Ultracompact optrode with integrated laser diode chips and SU-8 waveguides for optogenetic applications. In *IEEE 26th International Conference on Micro Electro Mechanical Systems (MEMS)* (Taipei, Taiwan, January 20–24).

Shin, G., Gomez, A.M., Al-Hasani, R., Jeong, Y.R., Kim, J., Xie, Z., Banks, A., Lee, S.M., Han, S.Y., Yoo, C.J., et al. (2017). Flexible near-field wireless optoelectronics as subdermal implants for broad applications in optogenetics. *Neuron* 93, 509–521.

Sim, J.Y., Haney, M.P., Park, S.I., McCall, J.G., and Jeong, J.-W. (2017). Microfluidic neural probes: in vivo tools for advancing neuroscience. *Lab. Chip* 17, 1406–1435.

Spiehl, S., Schumacher, A., Holtzman, T., Rich, P.D., Theobald, D.E., Dalley, J.W., Nouna, R., Messner, S., and Zengerle, R. (2012). An intracerebral drug delivery system for freely moving animals. *Biomed. Microdevices* 14, 799–809.

Stark, E., Koos, T., and Buzsáki, G. (2012). Diode probes for spatiotemporal optical control of multiple neurons in freely moving animals. *J. Neurophysiol.* 108, 349–363.

Steinmetz, N.A., Aydin, C., Lebedeva, A., Okun, M., Pachitariu, M., Bauza, M., Beau, M., Bhagat, J., Böhm, C., Broux, M., et al. (2020). Neuropixels 2.0: a miniaturized high-density probe for stable, long-term brain recordings. *Science* 372, eabf4588.

Tao, G., Abouraddy, A.F., Stolyarov, A.M., and Fink, Y. (2015). Multimaterial fibers. In *Lab-on-Fiber Technology*. Springer Series in Surface Sciences, 56, A. Cusano, M. Consales, A. Crescitelli, and A. Ricciardi, eds (Springer), pp. 1–26.

Tehovnik, E.J. (1996). Electrical stimulation of neural tissue to evoke behavioral responses. *J. Neurosci. Meth.* 65, 1–17.

Tien, L.W., Wu, F., Tang-Schomer, M.D., Yoon, E., Omenetto, F.G., and Kaplan, D.L. (2013). Silk as a

Multifunctional biomaterial substrate for reduced glial scarring around brain-penetrating electrodes. *Adv. Funct. Mater.* 23, 3185–3193.

Tsai, H.-C., Zhang, F., Adamantidis, A., Stuber, G.D., Bonci, A., de Lecea, L., and Deisseroth, K. (2009). Phasic firing in dopaminergic neurons is sufficient for behavioral conditioning. *Science* 324, 1080–1084.

Tye, K.M., and Deisseroth, K. (2012). Optogenetic investigation of neural circuits underlying brain disease in animal models. *Nat. Rev. Neurosci.* 13, 251–266.

Tye, K.M., Prakash, R., Kim, S.-Y., Fenno, L.E., Grosenick, L., Zarabi, H., Thompson, K.R., Gradinaru, V., Ramakrishnan, C., and Deisseroth, K. (2011). Amygdala circuitry mediating reversible and bidirectional control of anxiety. *Nature* 471, 358–362.

Vázquez-Guardado, A., Yang, Y., Bando, A.J., and Rogers, J.A. (2020). Recent advances in neurotechnologies with broad potential for neuroscience research. *Nat. Neurosci.* 23, 1522–1536.

Won, S.M., Song, E., Reeder, J.T., and Rogers, J.A. (2020). Emerging modalities and implantable technologies for neuromodulation. *Cell* 181, 115–135.

Wu, F., Stark, E., Im, M., Cho, I.-J., Yoon, E.-S., Buzsáki, G., Wise, K.D., and Yoon, E. (2013). An implantable neural probe with monolithically

integrated dielectric waveguide and recording electrodes for optogenetics applications. *J. Neural Eng.* 10, 056012.

Wu, F., Stark, E., Ku, P.-C., Wise, K.D., Buzsáki, G., and Yoon, E. (2015). Monolithically integrated  $\mu$ LEDs on silicon neural probes for high-resolution optogenetic studies in behaving animals. *Neuron* 88, 1136–1148.

Xie, C., Liu, J., Fu, T.-M., Dai, X., Zhou, W., and Lieber, C.M. (2015). Three-dimensional macroporous nanoelectronic networks as minimally invasive brain probes. *Nat. Mater.* 14, 1286–1292.

Yaman, M., Khudiyev, T., Ozgur, E., Kanik, M., Aktas, O., Ozgur, E.O., Deniz, H., Korkut, E., and Bayindir, M. (2011). Arrays of indefinitely long uniform nanowires and nanotubes. *Nat. Mater.* 10, 494–501.

Yin, Z., Kuang, D., Wang, S., Zheng, Z., Yadavalli, V.K., and Lu, S. (2018). Swellable silk fibroin microneedles for transdermal drug delivery. *Int. J. Biol. Macromol.* 106, 48–56.

Zhang, F., Prigge, M., Beyrière, F., Tsunoda, S.P., Mattis, J., Yizhar, O., Hegemann, P., and Deisseroth, K. (2008). Red-shifted optogenetic excitation: a tool for fast neural control derived from *Volvox carterii*. *Nat. Neurosci.* 11, 631–633.

Zhang, F., Gradinaru, V., Adamantidis, A.R., Durand, R., Airan, R.D., de Lecea, L., and Deisseroth, K. (2010). Optogenetic interrogation

of neural circuits: technology for probing mammalian brain structures. *Nat. Protoc.* 5, 439–456.

Zhang, Y., Castro, D.C., Han, Y., Wu, Y., Guo, H., Weng, Z., Xue, Y., Auser, J., Wang, X., Li, R., et al. (2019). Battery-free, lightweight, injectable microsystem for in vivo wireless pharmacology and optogenetics. *Proc. Natl. Acad. Sci. U S A* 116, 21427–21437.

Zhang, Q., Hu, S., Talay, R., Xiao, Z., Rosenberg, D., Liu, Y., Sun, G., Li, A., Caravan, B., Singh, A., et al. (2021). A prototype closed-loop brain-machine interface for the study and treatment of pain. *Nat. Biomed. Eng.* <https://doi.org/10.1038/s41551-021-00736-7>.

Zheng, K., Loh, K.Y., Wang, Y., Chen, Q., Fan, J., Jung, T., Nam, S.H., Suh, Y.D., and Liu, X. (2019). Recent advances in upconversion nanocrystals: expanding the kaleidoscopic toolbox for emerging applications. *Nano Today* 29, 100797.

Zorzos, A.N., Boyden, E.S., and Fonstad, C.G. (2010). Multiwaveguide implantable probe for light delivery to sets of distributed brain targets. *Opt. Lett.* 35, 4133–4135.

Zou, L., Tian, H., Guan, S., Ding, J., Gao, L., Wang, J., and Fang, Y. (2021). Self-assembled multifunctional neural probes for precise integration of optogenetics and electrophysiology. *Nat. Commun.* 12, 5871.